PAPER

Check for updates

Phase transition of recombinant fusion protein assemblies in macromolecularly crowded conditions†

Jooyong Shin, Yinhao Jia, Janani Sampath [ID] and Yeongseon Jang [ID] *

Artificial cells, synthetic analogues of living cells in both structure and function, have emerged as valuable tools for investigating the principles of life and for advanced applications. These artificial cells are constructed through the self-assembly of biological molecules and have been examined under macromolecularly crowded conditions. The dense environment of the intracellular cytoplasm or extracellular matrix is recapitulated by using macromolecules such as polyethylene glycol (PEG), with concentrations that typically range from 10 to 40% w/v. We investigate the self-assembly of recombinant fusion proteins composed of functionally folded globular protein and elastin-like polypeptide (ELP) into coacervates or vesicles to develop a potential artificial cell platform. Herein, we focus on understanding the phase transition of the recombinant fusion protein assemblies and vesicles in PEG-rich, macromolecularly crowded conditions by experiments and molecular dynamics simulations. It has been found that self-assembled protein vesicles undergo agglomeration in macromolecularly crowded conditions, where individual vesicles cluster to form larger aggregates. This is followed by the vesicle-to-coacervate transition and phase separation in the protein-rich particles. The PEG concentrations that induce the phase transition of the protein assemblies depend on the relative number of globular proteins at vesicle surfaces. This knowledge would be useful to provide engineering strategies for artificial cells in cell-like macromolecularly crowded conditions.

Introduction

Artificial cell research has been actively investigated in recent years, owing to its potential to better understand the complexity of life,[1,2] as well as its various potential applications in biotechnology, such as biosensors,[3] smart drug delivery,[4] and bioreactors.[5] For biotechnical applications, investigating artificial cells in cell-like environments is crucial for understanding cellular behavior and evaluating the adaptability of artificial cell functions in biological conditions. Thus, researchers have developed synthetic systems that mimic the structural and functional properties of living cells and their environments to investigate and predict the functions and behavior of artificial cells in biological conditions. One of the key properties of the cellular environment is macromolecular crowding, which indicates high concentrations of macromolecules in limited intracellular and extracellular space.[6,7]

Macromolecular crowding has been utilized to investigate cellular behavior since it has been shown to influence diverse biophysical and biochemical reactions, including *in vitro* transcription and translation,[8] enzyme kinetics,[9] and protein folding.[10] This is attributed to the presence of repulsive interactions within crowded environments, which induce spatial confinement and steric hindrance, thereby affecting the dynamics of molecular interactions.[11] In natural systems, membraneless organelles are formed by liquid–liquid phase separation of intrinsically disordered proteins in macromolecular crowding conditions.[12,13] Similarly, the macromolecularly crowded conditions can also impact some structural transitions of artificial cells, such as agglomerations[14] and phase separation,[15,16] due to the excluded volume effect. The excluded volume effect is a phenomenon in which the presence of one molecule cannot occupy space that is already occupied by other molecules.[17] Therefore, investigation of artificial cell platforms in macromolecularly crowded conditions is critical for advancing our understanding of synthetic particles' bio-adaptability.

To mimic *in vitro* macromolecularly crowding conditions, researchers have developed several methods, such as encapsulating crowding agents,[18] utilizing a densely packed hydrogel[19] or coacervate,[20] and developing confined spaces.[21] Among these

Department of Chemical Engineering, University of Florida, 1006 Center Drive, Gainesville, Florida, 32611, USA. E-mail: y.jang@ufl.edu

methods, encapsulating crowding agents is a widely used method to mimic macromolecularly crowded conditions due to several benefits, such as easy control of concentration and compatibility with a wide range of experimental techniques. Crowding agents are molecules that are added to a solution to mimic the effects of macromolecular crowding. Typical crowding agents are small, inert molecules such as dextran,[22] Ficoll,[23] or polyethylene glycol (PEG)[24] which do not participate in chemical reactions with other solutes but only create excluded volume. Among those candidates, PEG has been widely used as a crowding agent because of its biocompatibility,[25] high water solubility[26] and flexible chain structure.[27]

Towards developing an artificial cell platform, we have created globular protein vesicles (GPVs), self-assembled vesicles from recombinant fusion proteins.[28–31] The fusion protein building blocks are produced through recombinant technology, which is a powerful tool for the precise design of the protein building units and control over their self-assembly behavior. There are two key fusion proteins used for the self-assembly of globular protein vesicles; globular protein fused with a glutamic acid-rich leucine zipper (globule-Z_E) and an arginine-rich leucine zipper fused with elastin-like polypeptide (Z_R-ELP). These two complimentary leucine zipper pairs (Z_E/Z_R) show high binding affinity, which results in the formation of a globule-Z_E/Z_R-ELP fusion protein complex when these fusion proteins are mixed. ELP is a penta-repeated polypeptide derived from tropoelastin, Val-Pro-Gly-Xaa-Gly (VPGXG)$_n$, where any amino acid except proline (P) can replace Xaa.[32] ELP shows a thermally responsive inverse phase transition from hydrophilic below transition temperature to hydrophobic above the transition temperature due to lower critical solution temperature (LCST) behavior.[33] LCST of the ELP domain makes protein complexes behave as amphiphilic molecules above the transition temperature, composed of hydrophilic globular proteins and hydrophobic ELP tail, which results in self-assembly into a vesicle structure.

GPVs platforms have been considered as novel artificial cell platforms since functional globular proteins can be incorporated into synthetic vesicles membrane in benign conditions without chemical conjugation and the use of organic solvents, which affect protein activity. There are various studies of GPVs in membrane characterization,[30,31,34] the uses of different globular proteins[35] and drug delivery applications.[36] Previously, Jang et al. thoroughly investigated the self-assembly mechanisms,[30,34] nanostructures,[30] and physical properties[31] of GPVs using red fluorescent mCherry-Z_E or green fluorescent eGFP-Z_E, forming amphiphilic protein complexes with Z_R-ELP in water under varying temperatures and salt concentrations. However, the phase behavior of these recombinant protein assemblies and vesicles in macromolecular crowding environment is unknown and necessary for further development of advanced biotechnical applications. Therefore, herein, we investigated the phase behavior of pre-assembled GPVs in macromolecularly crowded conditions by adding a high concentration of crowding agents in the vesicle solution. The effects of a model crowding agent (PEG) concentration, the relative number and

types of bulky globular proteins at vesicle surfaces on the phase transition of GPVs have been studied experimentally and computationally using molecular dynamics simulation. This work would give fundamental and practical insights into the field of designing biomimetic materials towards artificial cells.

Experimental section

Materials

This work used two different types of recombinant fusion proteins: Z_R-ELP and globule-Z_E. Here, we used two different types of globular proteins, mCherry and enhanced green fluorescent protein (eGFP) fused with a glutamic acid-rich leucine zipper, respectively: i.e., mCherry-Z_E and eGFP-Z_E. Z_R-ELP is composed of an arginine-rich leucine zipper (Z_R) genetically fused with an elastin-like polypeptide (ELP, [(VPGVG)$_2$(VPGFG)(VPGVG)$_2$]$_5$). The expression and purification steps of Z_R-ELP and mCherry-Z_E are described in detail in the previous works, along with the protein sequences.[28,30,31] Poly(ethylene glycol) (PEG) ($\langle M_n \rangle$ = 8000 g mol^{-1}), used as a model crowding agent, are purchased from Sigma-Aldrich. FITC-PEG ($\langle M_n \rangle$ = 5000 g mol^{-1}), which are used for observing PEG location, are purchased from nanocs.

Monitoring GPVs phase behavior in macromolecularly crowded conditions

GPVs were prepared by mixing 120 μM of Z_R-ELP and 6 μM of globule-Z_E in concentrated PBS at different NaCl concentrations (i.e., 0.3 M for mCherry-Z_E, 0.91 M for eGFP-Z_E) on ice for 15 min, followed by incubation at 25 °C for 1 hour to induce self-assembly into vesicle structure. PEG molecules were dissolved in concentrated PBS, resulting in a final concentration ranging from 1 to 40 wt%. The phase behavior of GPVs were monitored through fluorescent and confocal microscopy (Carl Zeiss Observer 7 and LSM900) after mixing GPVs solution and various concentration of PEG solutions in same volume ratio.

Tuning the relative number of globular proteins on the vesicle surface

The relative number of globular proteins displayed on the vesicle surface can be tuned by changing the molar ratio of globule-Z_E (e.g., mCherry-Z_E and eGFP-Z_E) to Z_R-ELP in the vesicle formation solutions. With the fixed concentration of Z_R-ELP at 120 μM in PBS, globule-Z_E at a varied concentration from 0.6 to 6 μM were mixed to have molar ratios of globule-Z_E to Z_R-ELP from 0.005 to 0.05. GPVs made with different relative numbers of globular proteins were then mixed with PEG solution to have final 1–40 wt% PEG concentrations in the protein mixture solutions. The phase behavior of GPVs in the PEG-rich macromolecularly crowded conditions was observed through fluorescent microscopy over time.

Characterization of Z_R-ELP lower critical solution temperature (LCST) behavior in crowded conditions

To characterize hydrophobic interactions of ELP domains in the fusion protein building blocks as a function of temperature

in molecular crowding conditions, 100 μL of 60 μM Z_R-ELP solution with and without PEG solution was placed in microplate reader (Biotek Synergy H1). The optical density of the solutions at 400 nm was measured from 37 °C to 17 °C by decreasing temperature at cooling rate 1 °C min^{-1}.

Molecular dynamics simulation

All simulations were carried out using the GROMACS 2021.3 package,[37] along with the PLUMED 2.7.2 plugin[38] for enhanced sampling using metadynamics. A series of unbiased simulations were carried out to obtain the initial conformation of globular proteins (mCherry, and eGFP), and ELP. After the equilibration stage, the last frame was used for production runs. As the surface charges play an essential role in protein–protein interactions, (based on the preliminary simulations, which allow proteins to interact from different directions, the proteins prefer to interact and bind to each other according to the opposite charge of the surface.) we employ the adaptive Poisson–Boltzmann solver (APBS)[39] method on single proteins to obtain the electrostatic distribution of each protein surface. Then, for the metadynamics simulations, the starting configuration was generated by aligning the two proteins based on the APBS result. The positively charged region of the first protein is aligned to the negatively charged region of the second protein, as shown in Fig. S4 in the ESI.† Next, one of the proteins is fixed by applying a position restraint on the backbone atoms along x-, y-, and z-axis, and the other protein is allowed to move only along the x-axis, by an applying position restraint on the backbone atoms along the y- and z-axis. We believe that this is the optimal configuration for generating a one-dimension free energy profile of inter-protein interactions. Well-tempered metadynamics (MetaD)[40] is employed to study the binding free energy between mCherr–mCherry, eGFP–eGFP, mCherry–ELP, and ELP–ELP. Center of mass distance (COM) is used as the collective variable (CV) to apply bias to. For each system, the simulations were carried out at least for 200 ns, and the convergence of the simulation is ensured by monitoring the evolution of the free energy, as well as the average error on the free-energy profile using block averaging methods. The demonstration of convergence was included in the ESI.†

Result and discussion

Macromolecular crowding-induced agglomeration of GPVs

GPVs were made through self-assembly of recombinant fusion proteins, globule-Z_E and Z_R-ELP. Two fusion proteins form a protein complex via high binding affinity of leucine zipper pairs (Z_E/Z_R, $K_d \approx 10^{-15}$ M) and self-assemble into hollow vesicle structure at 25 °C, which is above the transition temperature of ELP.[28,30] Fluorescent globular proteins, mCherry and enhanced green fluorescent protein (eGFP), are utilized as a hydrophilic protein head in the globule-Z_E/Z_R-ELP protein building block complex and a model functionally folded globular proteins displayed at the self-assembled protein vesicle membranes.
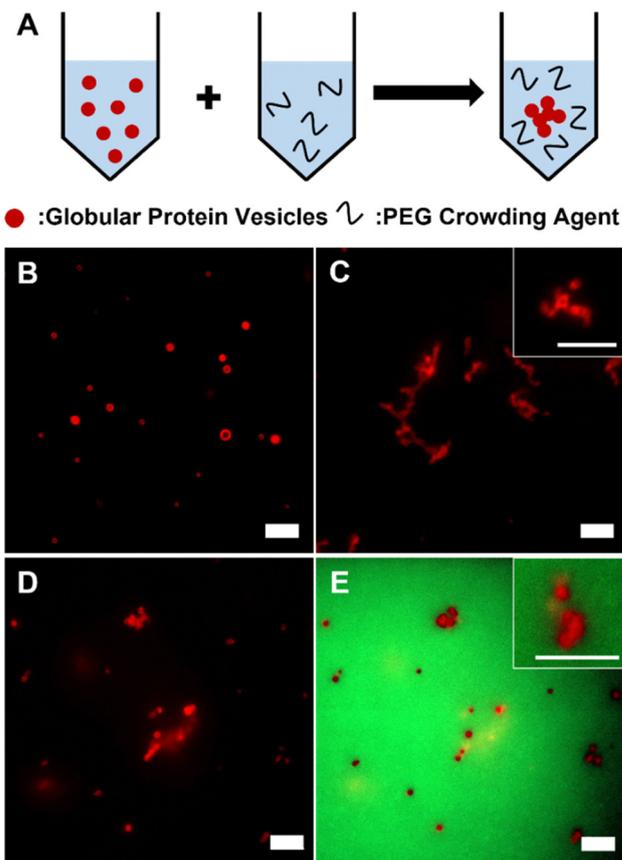

Fig. 1 (A) A schematic illustration to show macromolecular crowding-induced agglomeration of GPVs. GPVs were dispersed (B) in PBS solution without PEG, (C) in PEG 20 wt% mixture solution, and (D and E) in PEG 20 wt% mixed with 1% of FITC–PEG solution monitored under red fluorescent channel only (D) and both red and green fluorescent channels (E). Red and green fluorescent signals come from mCherry of GPV building blocks and FITC conjugated to PEG, respectively. Scales bars are 5 μm.

To investigate the phase behavior of GPVs in macromolecular crowded conditions that simulate the intracellular environment in vitro, a widely used model crowding agent, PEG, was added into the pre-assembled GPV solutions (Fig. 1A). In this work, we varied PEG concentrations from 1 wt% to 40 wt% as typical macromolecular crowding agent concentration is between 200 and 400 mg mL^{-1}.[41] Without PEG in the solutions, GPVs are distributed separately over the solution (Fig. 1B). However, after adding 20 wt% of PEG into the solution, GPVs begin to form agglomeration, a process where individual vesicles congregate together to form larger clusters, due to the excluded volume effect (Fig. 1C). This effect arises because PEG polymer chains have finite sizes and are unable to occupy the same space with other molecules simultaneously.[42,43] PEG molecules at high concentrations are distributed throughout the solution by taking up the solvent volume. In this regard, the addition of PEG creates excluded volume effect to decrease the available volume of solvents for GPVs, thus, induces the formation of agglomeration of GPVs. To confirm the PEG-induced excluded volume effect, we monitored the location of PEG during GPV agglomeration by adding 1% of green fluorescent, fluorescein isothiocyanate-conjugated

PEG (FITC-PEG) into total PEG concentration at 20 wt% (Fig. 1D and E). As a result, FITC-PEG was distributed outside of GPVs, indicating that PEG only creates excluded volume effect without having any specific interaction with fusion protein building blocks.

The effect of depletion force on the GPV agglomeration in macromolecular crowded conditions

The theoretical approach of GPVs agglomeration can further be explained by the idea of depletion force, which is a concept widely utilized in colloidal physics. Depletion force is a type of attractive force that arises between colloidal particles in a solution because of the existence of crowding agents nearby.[44] When two GPVs get closer to each other, their excluded volumes are overlapped, which results in the exclusion of crowding agents from interparticle-overlapped regions. The concentration gradient of crowding agents induces osmotic pressure, which is thought to be a driving force of agglomeration of GPVs in crowded conditions.

Agglomeration of GPVs, regardless of globular protein types, either mCherry or eGFP, was observed in macromolecular crowded conditions (Fig. 2). Interestingly, we found the critical PEG concentration, which is defined as the concentration at that GPVs agglomeration begins, would slightly defer by the types of globular proteins. It is reported that the strength of depletion forces increases with increasing concentration of crowding agents because the high concentration of crowding agents can induce a stronger concentration gradient between the interparticle region and surrounding.[44] Below the critical PEG concentration, depletion force is not enough to induce GPVs agglomeration; thus, it is observed that GPVs exist individually in dilute PEG solutions. As the PEG concentration increases in solutions, mCherry–GPVs start to form

agglomeration above 6 wt% PEG, while eGFP–GPVs agglomerations are formed at 2 wt% PEG. At PEG concentrations higher than the critical point, no significant difference in GPVs agglomeration made of mCherry and eGFP fusion proteins was observed. mCherry proteins present electrostatic repulsive forces with each other due to slightly negative charged surface potential, while eGFP have attractive forces with each other due to dimerization preference.[28] Thus, eGFP–GPVs are easy to present agglomeration behavior in lower PEG critical concentrations than mCherry–GPVs.

The effect of depletion force on the GPV agglomeration in macromolecular crowded conditions was further studied by altering molar ratios of globule-Z_E to Z_R-ELP fusion proteins to tune the relative number of displayed globular proteins on the vesicle surface. GPVs made with the lower ratio of globule-Z_E to fixed Z_R-ELP proteins have fewer globular proteins exposed on the surface. We hypothesized the decrease in the relative number of globular proteins on the vesicle membrane would reduce the excluded volume of the vesicle surface, resulting in mitigation of agglomerating GPVs in macromolecularly crowded conditions (Scheme 1).

To test this hypothesis, we prepared GPVs at three different molar ratios of globule-Z_E to Z_R-ELP (*i.e.*, 0.005, 0.01, 0.05) and monitored critical PEG concentration that starts to induce agglomeration of GPVs through fluorescent microscopy. As shown in Fig. 3, the smaller relative number of mCherry proteins displayed on the GPV surface requires a higher PEG concentration to form agglomeration. For example, GPVs made with mCherry-Z_E protein at 0.005 molar ratio to Z_R-ELP do not form agglomeration even in a 40 wt% PEG solution. This result indicates that the lower mCherry protein on the GPVs surface mitigates the tendency of agglomeration due to the decreased excluded volume on the surface.
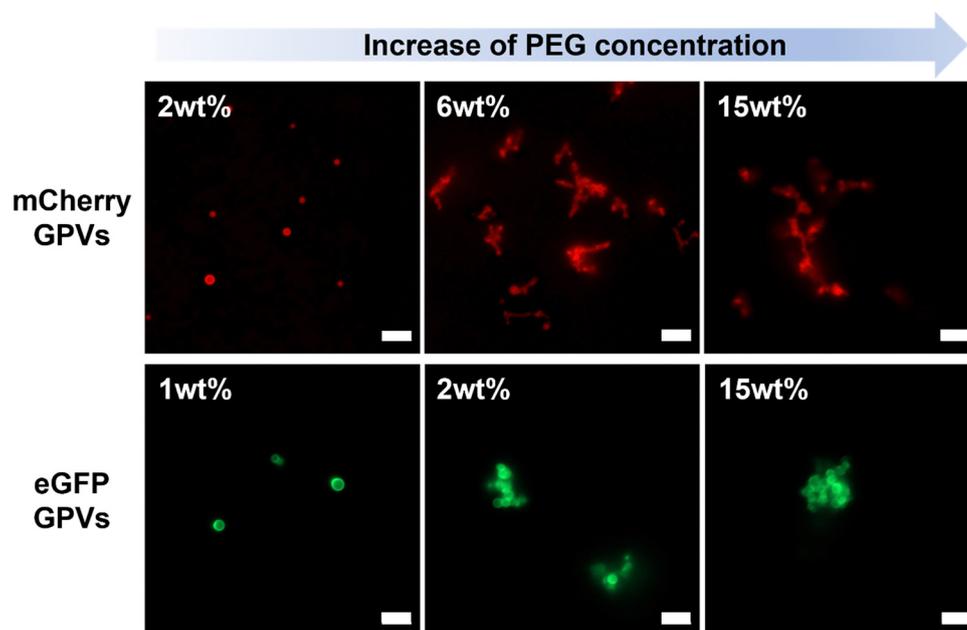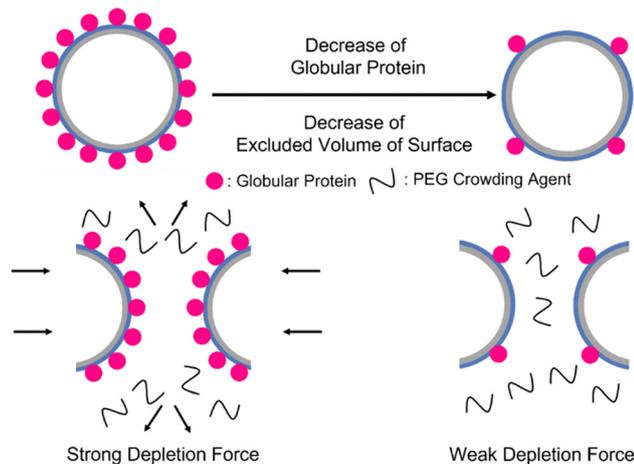

Fig. 2 Two different types of GPVs in PEG solutions at varied concentrations. All scale bars are 5 μm.

Scheme 1 Illustration of decrease in the number of globular proteins on the vesicle surface. High number of globular proteins induce stronger depletion force to form GPVs agglomeration.

To confirm this phenomenon with other types of globular protein, mCherry protein was replaced by eGFP (Fig. 4). The eGFP–GPVs showed a similar trend to the mCherry–GPVs. The lower relative number of eGFPs on the vesicle surface requires higher PEG concentrations to form agglomeration. This result suggests engineering strategies to mitigate GPVs agglomeration in macromolecularly crowding conditions by tuning depletion force on the vesicle surface, which can be utilized in various types of GPVs for diverse potential applications.

By utilizing metadynamics calculations, we find that the binding free energy between eGFP and eGFP is approximately -19.8 kJ mol^{-1}, higher than that of mCherry and mCherry, which is approximately -10.6 kJ mol^{-1} (Fig. 5). This finding

suggests a greater propensity for eGFP molecules to interact with one another and form stable dimer structures when situated at close distances. This result is in agreement with experimental observations, wherein eGFP–GPVs exhibit a lower critical PEG concentration than mCherry–GPVs for triggering agglomeration under the same low molar ratio of globular protein-Z_E to Z_R-ELP.

Kinetics in the phase transition and separation of protein assemblies in the macromolecular crowding-induced concentrated conditions

GPVs agglomeration was observed within minutes upon addition of a high concentration of PEG solution. However, after a few hours, the agglomerated GPVs changed into particulates that show sub-domain phase separation (Fig. 6A). The phase separation was characterized by observing the sub-domains formation of distinct mCherry-rich and mCherry-poor regions in protein particulates, which were stable over a week.

Previously, we found that the agglomeration of GPVs is ultimately confined by the PEG crowding agent nearby. This will result in the increase of local concentrations of fusion proteins in the limited space. When local concentrations of the amphiphilic globule-Z_E/Z_R-ELP fusion proteins are bigger than disorder–order transition concentrations, we anticipate the collapse of vesicle structure and phase separation between the globular proteins-rich domain and ELP-rich domain, as shown in Fig. 6A. The intensity profiles of mCherry in the droplets assembled from the fusion proteins in PEG-rich solutions clearly demonstrate the phase separation between ELP and mCherry domains (Fig. S1, ESI†). This phase transition occurs in 6 hours after addition of PEG in the GPV solutions. We used FITC-PEG to find the location of PEG molecules during the vesicle-to-coacervate phase transition as well as
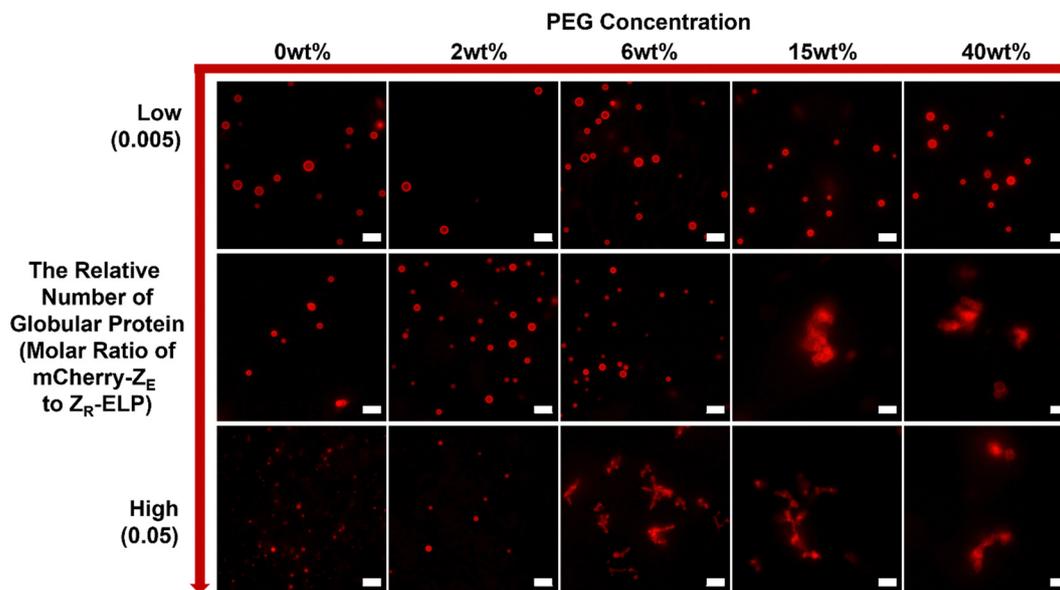

Fig. 3 Phase behavior of GPVs with different relative number of mCherry proteins on the vesicle surfaces (*i.e.*, molar ratios of mCherry-Z_E to Z_R-ELP are 0.005 (low; upper row), 0.01 (middle row), and 0.05 (high; bottom row)) in various PEG concentrations. All scale bars are 5 μm.
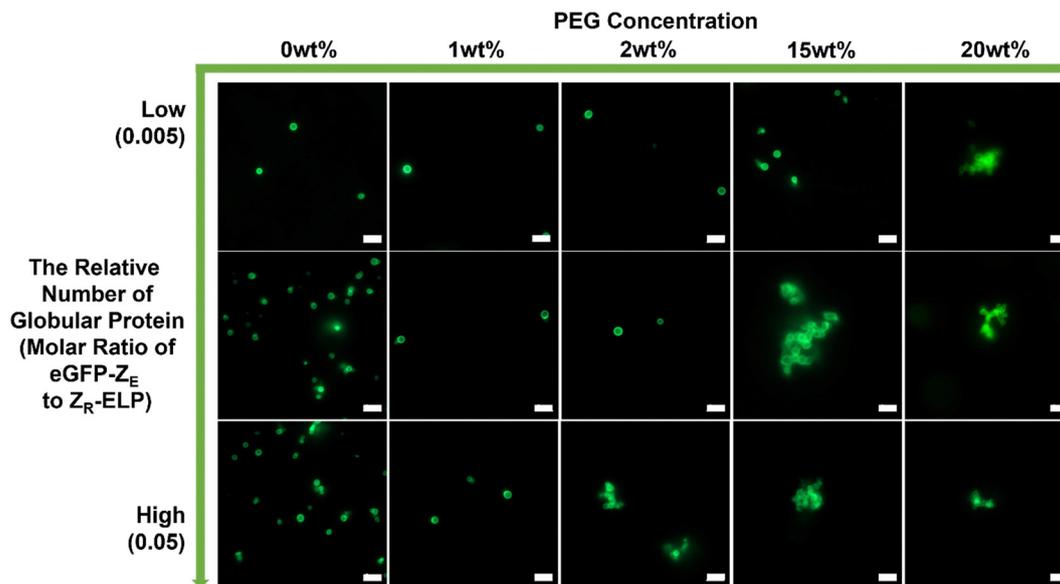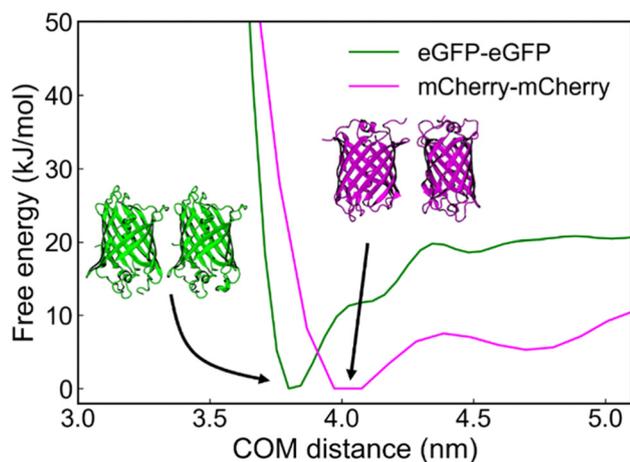
Fig. 4 Phase behavior of GPVs with different relative number of eGFP on the vesicle surface (*i.e.*, molar ratio of eGFP-Z_E to Z_R-ELP are 0.005 (low; upper row), 0.01 (middle row) and 0.05 (high; bottom row)) in various PEG concentrations. All scale bars are 5 μm.

Fig. 5 Free-energy profile as a function of center-of-mass (COM) distance between eGFP–eGFP, and mCherry–mCherry.

Fig. 6 (A) Phase separation of mCherry and ELP domains observed in a protein-rich assemblies, made from PEG-induced agglomeration and the vesicle-to-coacervate transitions. (B) Green fluorescent signal from FITC-PEG surrounding phase-separated protein assemblies. (C) The turbidity changes of ELP fusion protein solutions in dilute and concentrated PEG conditions. All scale bars are 5 μm.

the phase separation of mCherry and ELP domains in the protein-rich coacervate particles. PEG crowding agents are located outside the phase-separated particles (Fig. 6B), which indicates that the increase in the local concentration of fusion proteins inside the protein-rich droplets results in phase separation between mCherry and ELP domains due to the desolvation of ELP domains and the discrepancy of attraction forces between mCherry and ELP. Similarly, it is reported that mCherry–ELP fusion proteins formed ordered nanostructure in concentrated conditions above the disorder–order concentration.[45] The size of the droplets exhibits a wide dispersity and is larger than that of GPVs, since numerous GPVs cluster together to form agglomerations that coalesce into protein droplets (Fig. S2, ESI†).
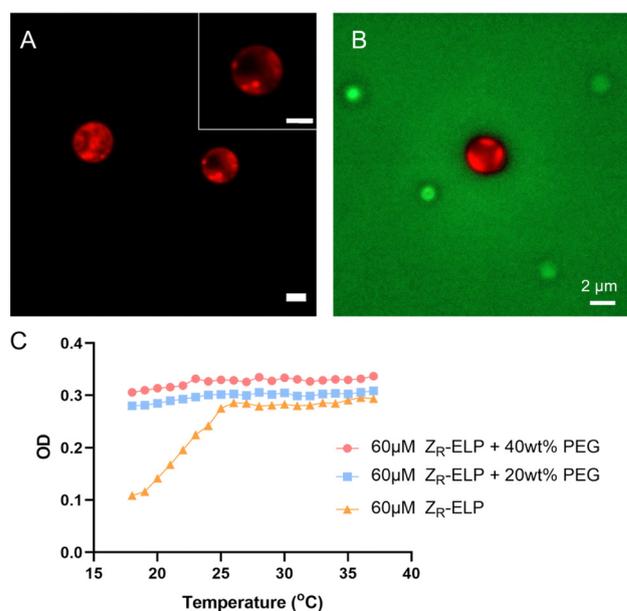
The main driving force behind the transition of agglomerated GPVs into phase-separated protein assemblies is thought to be the increased hydrophobic interaction between ELPs in highly concentrated solutions, a result of macromolecular crowding. Fig. 6C shows the optical density of ELP solutions in dilute and concentrated PEG conditions as a function of

temperature. In dilute solutions (*e.g.*, no macromolecular crowded conditions, 10–120 μM Z_R-ELP solutions), the soluble to insoluble transition of ELPs due to their LCST behavior was clearly observed with the increasing turbidity profiles upon heating, indicating that the increased ELP hydrophobic interactions in water formed two phases at the temperatures above transition temperatures.[30] We also confirmed that the ELP phase transition is reversible to return to soluble phase upon cooling in no PEG conditions. However, ELP in macromolecular crowding solutions (20 and 40 wt%) did not show a decrease in optical density with the decrease in temperature. This result implies that macromolecular crowded conditions prevent the ELP chain from stretching out to be dissolved in aqueous solution due to excluded volume effect, leading to the enhanced hydrophobic interaction between ELP fusion proteins. As the local concentration of fusion proteins is increased during the GPV agglomeration-induced protein-rich droplet formations by PEG molecules surrounding, the hydrophobic interaction of ELP is increased and ELP proteins become immiscible with hydrophilic mCherry. More detailed investigation of the phase separation at the nanometer scale warrants future investigation by using scattering techniques, which is beyond the current study.

Molecular dynamics simulation to estimate the interaction between mCherry–mCherry, ELP–ELP, and mCherry–ELP in protein assemblies.

To gain a deeper understanding of the driving forces behind the sub-domain phase separation of mCherry and ELP complex assemblies after GPV agglomeration by PEG addition, we employed metadynamics to calculate the binding free energy as a function of the center-of-mass (COM) distance between mCherry–ELP protein pairs (Fig. 7). All simulation details, including simulation setup for well-tempered metadynamics

Fig. 7 Free-energy profile as a function of center-of-mass (COM) distance between mCherry–mCherry, mCherry–ELP, and ELP–ELP.

(Table S1, ESI†), convergence assessment showing last 40 ns free energy profile changes (Fig. S3, ESI†) and average error on free-energy profiles with varying block size (Fig. S4, ESI†) for each protein components, and simulation initial conformation alignment (Fig. S5, ESI†) are summarized in more detail in ESI.† As a result, among all the protein–protein interactions analyzed, ELP–ELP demonstrated the highest binding free energy of −10.1 kJ mol^{-1}, followed by mCherry–mCherry with a free energy of −7.5 kJ mol^{-1}, and finally mCherry–ELP exhibited the weakest interaction of −5.7 kJ mol^{-1}.

This MD simulation result suggests that ELPs have a preference for interacting with other ELPs at close proximity, while mCherrys show an inclination towards binding with other mCherrys. Given the preferential nature of these interactions, the weaker interaction between mCherry and ELP contributes to the phase separation between mCherry and ELP aggregates. This ultimately supports the observed phase separation under crowded conditions.

Conclusion

We investigated the phase behavior of recombinant fusion protein vesicles and assemblies in macromolecularly crowded conditions, which were created by adding high concentrated model crowding agents, PEG. We found that excluded volume effect of crowding agents induced the agglomeration and phase transition of GPVs, in which the relative number of bulky globular proteins at the vesicle membranes plays a critical role due to the depletion effect. When PEG concentration is high enough to induce depletion force between vesicles, GPVs agglomerate, which can be mitigated by reducing the relative number of globular proteins on vesicle surfaces. Altering globular protein types from mCherry to eGFP exhibited similar trends, which demonstrated that we could apply the same engineering strategies on different globular protein vesicles to mitigate the agglomeration. When the local concentration of fusion proteins in the confined space, such as protein-rich coacervate droplets, increases more than the disorder–order transition concentration, the agglomerated GPVs undergo further phase-separation. The phase separation inside the fusion protein assemblies at high local concentrations is based on the increased immiscibility between mCherry and ELP in macromolecularly crowded conditions. Our experimental and computational simulations confirmed that hydrophobic interaction of ELP fusion proteins is enforced in macromolecularly crowded conditions. This work to investigate the phase behavior of recombinant fusion proteins and their assembly in cell-like crowded conditions, including agglomeration, coacervate-to-vesicle transition, and phase separation between protein domains would provide novel insights and engineering strategies for developing highly potential protein-displaying vesicles towards artificial cell and biotechnical applications.

Author contributions

The manuscript was written through contributions of all authors. All authors have given approval to the final version of the manuscript.
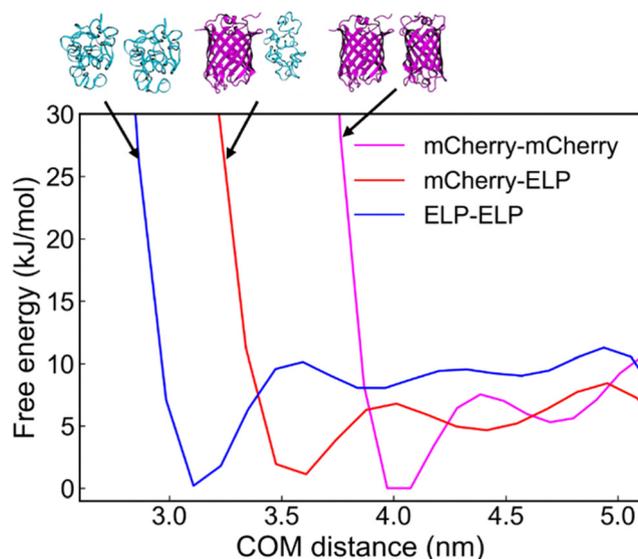
Conflicts of interest

There are no conflicts to declare.

Acknowledgements

References

1 D. A. Hammer and N. P. Kamat, Towards an artificial cell, *FEBS Lett.*, 2012, **586**(18), 2882–2890.

2 A. Salehi-Reyhani, O. Ces and Y. Elani, Artificial cell mimics as simplified models for the study of cell biology, *Exp. Biol. Med.*, 2017, **242**(13), 1309–1317.

3 K. P. Adamala, D. A. Martin-Alarcon, K. R. Guthrie-Honea and E. S. Boyden, Engineering genetic circuit interactions within and between synthetic minimal cells, *Nat. Chem.*, 2017, **9**(5), 431–439.

4 H. Kang, M. B. O'Donoghue, H. Liu and W. Tan, A liposome-based nanostructure for aptamer directed delivery, *Chem. Commun.*, 2010, **46**(2), 249–251.

5 N.-N. Deng, M. A. Vibhute, L. Zheng, H. Zhao, M. Yelleswarapu and W. T. Huck, Macromolecularly crowded protocells from reversibly shrinking monodisperse liposomes, *J. Am. Chem. Soc.*, 2018, **140**(24), 7399–7402.

6 D. Miyoshi and N. Sugimoto, Molecular crowding effects on structure and stability of DNA, *Biochimie*, 2008, **90**(7), 1040–1051.

7 A. A. André and E. Spruijt, Liquid–liquid phase separation in crowded environments, *Int. J. Mol. Sci.*, 2020, **21**(16), 5908.

8 M. A. Vibhute, M. H. Schaap, R. J. Maas, F. H. Nelissen, E. Spruijt, H. A. Heus, M. M. Hansen and W. T. Huck, Transcription and translation in cytomimetic protocells perform most efficiently at distinct macromolecular crowding conditions, *ACS Synth. Biol.*, 2020, **9**(10), 2797–2807.

9 N. A. Yewdall, B. C. Buddingh, W. J. Altenburg, S. B. Timmermans, D. F. Vervoort, L. K. Abdelmohsen, A. F. Mason and J. C. van Hest, Physicochemical characterization of polymer-stabilized Coacervate protocells, *ChemBioChem*, 2019, **20**(20), 2643–2652.

10 A. Christiansen, Q. Wang, M. S. Cheung and P. Wittung-Stafshede, Effects of macromolecular crowding agents on protein folding in vitro and in silico, *Biophys. Rev.*, 2013, **5**, 137–145.

11 A. P. Minton, Implications of macromolecular crowding for protein assembly, *Curr. Opin. Struct. Biol.*, 2000, **10**(1), 34–39.

12 V. N. Uversky, Intrinsically disordered proteins in over-crowded milieu: Membrane-less organelles, phase separation, and intrinsic disorder, *Curr. Opin. Struct. Biol.*, 2017, **44**, 18–30.

13 S.-P. Wei, Z.-G. Qian, C.-F. Hu, F. Pan, M.-T. Chen, S. Y. Lee and X.-X. Xia, Formation and functionalization of membraneless compartments in Escherichia coli, *Nat. Chem. Biol.*, 2020, **16**(10), 1143–1148.

14 L. Zhang, N. Burns, M. Jordan, L. Jayasinghe and P. Guo, Macromolecule sensing and tumor biomarker detection by harnessing terminal size and hydrophobicity of viral DNA packaging motor channels into membranes and flow cells. *Biomaterials*, *Science*, 2022, **10**(1), 167–177.

15 K. Kohata and D. Miyoshi, RNA phase separation–mediated direction of molecular trafficking under conditions of molecular crowding, *Biophys. Rev.*, 2020, **12**(3), 669–676.

16 S. Park, R. Barnes, Y. Lin, B.-J. Jeon, S. Najafi, K. T. Delaney, G. H. Fredrickson, J.-E. Shea, D. S. Hwang and S. Han, Dehydration entropy drives liquid-liquid phase separation by molecular crowding, *Commun. Chem.*, 2020, **3**(1), 83.

17 D. Gnutt, M. Gao, O. Brylski, M. Heyden and S. Ebbinghaus, Excluded-volume effects in living cells, *Angew. Chem., Int. Ed.*, 2015, **54**(8), 2548–2551.

18 K. Totani, Y. Ihara, I. Matsuo and Y. Ito, Effects of macromolecular crowding on glycoprotein processing enzymes, *J. Am. Chem. Soc.*, 2008, **130**(6), 2101–2107.

19 J.-Y. Dewavrin, N. Hamzavi, V. Shim and M. Raghunath, Tuning the architecture of three-dimensional collagen hydrogels by physiological macromolecular crowding, *Acta Biomater.*, 2014, **10**(10), 4351–4359.

20 Y. Zhang, Y. Chen, X. Yang, X. He, M. Li, S. Liu, K. Wang, J. Liu and S. Mann, Giant coacervate vesicles as an integrated approach to cytomimetic modeling, *J. Am. Chem. Soc.*, 2021, **143**(7), 2866–2874.

21 C. Jeon, Y. Jung and B.-Y. Ha, Effects of molecular crowding and confinement on the spatial organization of a biopolymer, *Soft Matter*, 2016, **12**(47), 9436–9450.

22 I. Pastor, L. Pitulice, C. Balcells, E. Vilaseca, S. Madurga, A. Isvoran, M. Cascante and F. Mas, Effect of crowding by Dextrans in enzymatic reactions, *Biophys. Chem.*, 2014, **185**, 8–13.

23 Y. Wang, H. He and S. Li, Effect of Ficoll 70 on thermal stability and structure of creatine kinase, *Biochemistry*, 2010, **75**, 648–654.

24 V. Nolan, J. M. Sánchez and M. A. Perillo, PEG-induced molecular crowding leads to a relaxed conformation, higher thermal stability and lower catalytic efficiency of Escherichia coli β-galactosidase, *Colloids Surf., B*, 2015, **136**, 1202–1206.

25 K. Bjugstad, D. Redmond Jr, K. Lampe, D. Kern, J. Sladek Jr and M. Mahoney, Biocompatibility of PEG-based hydrogels in primate brain, *Cell Transplant.*, 2008, **17**(4), 409–415.

26 A. A. André, N. A. Yewdall and E. Spruijt, Crowding-induced phase separation and gelling by co-condensation of PEG in NPM1-rRNA condensates, *Biophys. J.*, 2023, **122**(2), 397–407.

27 N. Tokuriki, M. Kinjo, S. Negi, M. Hoshino, Y. Goto, I. Urabe and T. Yomo, Protein folding by the effects of macromolecular crowding, *Protein Sci.*, 2004, **13**(1), 125–133.

28 W. M. Park and J. A. Champion, Thermally triggered self-assembly of folded proteins into vesicles, *J. Am. Chem. Soc.*, 2014, **136**(52), 17906–17909.

29 Y. Jang and J. A. Champion, Self-assembled materials made from functional recombinant proteins, *Acc. Chem. Res.*, 2016, **49**(10), 2188–2198.

30 Y. Jang, W. T. Choi, W. T. Heller, Z. Ke, E. R. Wright and J. A. Champion, Engineering globular protein vesicles through tunable self-assembly of recombinant fusion proteins, *Small*, 2017, **13**(36), 1700399.

31 R. Tan, J. Shin, J. Heo, B. D. Cole, J. Hong and Y. Jang, Tuning the Structural Integrity and Mechanical Properties of Globular Protein Vesicles by Blending Crosslinkable and NonCrosslinkable Building Blocks, *Biomacromolecules*, 2020, **21**(10), 4336–4344.

32 Y. N. Zhang, R. K. Avery, Q. Vallmajo-Martin, A. Assmann, A. Vegh, A. Memic, B. D. Olsen, N. Annabi and A. Khademhosseini, A highly elastic and rapidly crosslinkable elastin-like polypeptide-based hydrogel for biomedical applications, *Adv. Funct. Mater.*, 2015, **25**(30), 4814–4826.

33 N. K. Li, F. G. Quiroz, C. K. Hall, A. Chilkoti and Y. G. Yingling, Molecular description of the LCST behavior of an elastin-like polypeptide, *Biomacromolecules*, 2014, **15**(10), 3522–3530.

34 Y. Jang, M.-C. Hsieh, D. Dautel, S. Guo, M. A. Grover and J. A. Champion, Understanding the coacervate-to-vesicle transition of globular fusion proteins to engineer protein vesicle size and membrane heterogeneity, *Biomacromolecules*, 2019, **20**(9), 3494–3503.

35 D. R. Dautel and J. A. Champion, Protein vesicles self-assembled from functional globular proteins with different charge and size, *Biomacromolecules*, 2020, **22**(1), 116–125.

36 Y. Li and J. A. Champion, Photocrosslinked, tunable protein vesicles for drug delivery applications, *Adv. Healthcare Mater.*, 2021, **10**(15), 2001810.

37 M. J. Abraham, T. Murtola, R. Schulz, S. Páll, J. C. Smith, B. Hess and E. Lindahl, GROMACS: High performance molecular simulations through multi-level parallelism from laptops to supercomputers, *SoftwareX*, 2015, **1**, 19–25.

38 G. A. Tribello, M. Bonomi, D. Branduardi, C. Camilloni and G. Bussi, PLUMED 2: New feathers for an old bird, *Comput. Phys. Commun.*, 2014, **185**(2), 604–613.

39 E. Jurrus, D. Engel, K. Star, K. Monson, J. Brandi, L. E. Felberg, D. H. Brookes, L. Wilson, J. Chen and K. Liles, Improvements to the APBS biomolecular solvation software suite, *Protein Sci.*, 2018, **27**(1), 112–128.

40 A. Barducci, G. Bussi and M. Parrinello, Well-tempered metadynamics: a smoothly converging and tunable free-energy method, *Phys. Rev. Lett.*, 2008, **100**(2), 020603.

41 S. B. Zimmerman and S. O. Trach, Estimation of macromolecule concentrations and excluded volume effects for the cytoplasm of Escherichia coli, *J. Mol. Biol.*, 1991, **222**(3), 599–620.

42 I. M. Kuznetsova, B. Y. Zaslavsky, L. Breydo, K. K. Turoverov and V. N. Uversky, Beyond the excluded volume effects: mechanistic complexity of the crowded milieu, *Molecules*, 2015, **20**(1), 1377–1409.

43 H.-X. Zhou, G. Rivas and A. P. Minton, Macromolecular crowding and confinement: biochemical, biophysical, and potential physiological consequences, *Annu. Rev. Biophys.*, 2008, **37**, 375–397.

44 G. Ping, G. Yang and J.-M. Yuan, Depletion force from macromolecular crowding enhances mechanical stability of protein molecules, *Polymer*, 2006, **47**(7), 2564–2570.

45 G. Qin, M. J. Glassman, C. N. Lam, D. Chang, E. Schaible, A. Hexemer and B. D. Olsen, Topological Effects on Globular Protein-ELP Fusion Block Copolymer Self-Assembly, *Adv. Funct. Mater.*, 2015, **25**(5), 729–738.